ACTA IMEKO
ISSN: 2221-870X
September 2025, Volume 14, Number 3, 1 - 11

Characterization of a global navigation satellite system's vertical measurement system for sea state monitoring

Mohamad Khalil[1], Francesco Crenna[1], Giovanni Battista Rossi[1]

[1] *Department of Mechanical, Energy, Management and Transport Engineering – DIME, University of Genoa, Italy*

ABSTRACT
This study investigates the effectiveness of Global Navigation Satellite System (GNSS) signals for measuring vertical displacement (or heave) in dry conditions, using a controlled pendulum to create a wave-like motion. The experiment was conducted using three GNSS receivers operating in different measurement modes: Single Point (SP), Differential GNSS (DGNSS), and Real Time Kinematics (RTK). An Inertial Navigation System (INS), with high precision for navigation applications, was previously verified, then used as a reference in the experiment. The vertical motion, or heave, was obtained from the three receivers, considering the position measurements or by integrating the velocity measurements over time. Results indicate that GNSS velocity measurements are effective, but precision is limited by sensor characteristics. The RTK mode provided the highest accuracy, with a deviation of 2.5 % from the reference signal, followed by DGNSS at 3.5 %, and SP mode at 4 %. Altitude-based heave estimations showed similar trends, with RTK being the most accurate. However, signal loss in the RTK mode poses challenges in the management of measurement data, impacting measurement stability. The findings suggest that, while GNSS-based heave estimation is feasible, improvements in velocity precision and correction signal reliability are necessary for enhanced accuracy. This study provides insights into GNSS-based motion measurement techniques, highlighting their potential and limitations in marine applications.

Section: RESEARCH PAPER

Keywords: GNSS; sea state estimation; inertial sensors; directional spectrum

Citation: M. Khalil, F. Crenna, G. B. Rossi, Characterization of a global navigation satellite system's vertical measurement system for sea state monitoring, Acta IMEKO, vol. 14 (2025) no. 3, pp. 1-11. DOI: 10.21014/actaimeko.v14i3.2077

Section Editor: Andrea Scorza, University Roma Tre, Italy

Received February 18, 2025; **In final form** July 29, 2025; **Published** September 2025

Funding: Partially funded by the European Union - NextGenerationEU and by the Ministry of University and Research (MUR), National Recovery and Resilience Plan (NRRP), Mission 4, Component 2, Investment 1.5, project "RAISE - Robotics and AI for Socio-economic Empowerment" (ECS00000035).

Corresponding author: Mohamad Khalil, e-mail: mohamad.khalil01@edu.unige.it

1. INTRODUCTION

The measurement of the sea state includes several parameters that characterize the sea waves, such as wave height or heave, wave direction, wave period, and others. Indeed, it is a complex measurement, and it can be obtained directly or indirectly. In [1], the theory behind direct and indirect measurements is considered, and the importance of the mathematical modelling of the measurement process is demonstrated to be a key issue in measurement science and for indirect measurements. Direct measurements of the sea state are performed by wave buoys or other sources, such as onshore radars or oceanographic satellites [2]. An indirect possibility for sea-state estimation is offered by the measurement of the response of a ship during navigation, due to the interaction with sea waves [3]. In that case, modelling is even more important.

When considering the motion of the ship due to the sea waves, the Response Amplitude Operator of the specific vessel must be considered. When the vessel, through the wave buoy analogy, is considered as a wave buoy to estimate the sea state parameters, the inverse model must be considered, since the goal is to estimate the characteristics of the sea waves causing the vessel's motion [4]. To this purpose, vessel motion during navigation is measured onboard, for example by inertial sensors [5]. The inverse model is fed with three main motion parameters: the vessel's vertical movement or heave, and the angular movement along two perpendicular axes: roll and pitch. In [6], it appeared that utilizing the wave buoy analogy is a cost-effective approach for sea state estimating derived the from ship's motion, and the restricted isometry property method to evaluate the analogy was introduced, by combining multiple measured data from different ship boards having different geometries and using

different headings, to improve the accuracy of the wave buoy analogy.

The displacement on the vertical axis of the centre of gravity of the vessel is one of the fundamental parameters for the estimation of the sea state. Since it is often difficult to install a sensor exactly there, its motion can be reconstructed from a measurement in a convenient position along the vessel, then considering it as a rigid body, the orientation of which is also measured. For this purpose, a good-quality Inertial Measurement Unit (IMU) can be the best choice [7], even if some redundancy can improve both the displacement and the angular measurement accuracies, as presented in [8], where two IMUs were installed, on a vessel's stern and bow, in the front and back of the body ship, for increasing the accuracy of the measurement. To sum up, IMUs are used to feed the wave buoy analogy with the vertical displacement, or vessel heave, and its orientation along the X (pitch) and Y (roll) axis.

The diffusion of Global Navigation Satellite System receivers, at the consumer level also, provides a further possibility to measure some of the required parameters on a vessel or on a wave buoy. For example, Datawell has introduced in the market a new wave buoy model, DWR-G, that is based on the GNSS technology for measuring the sea parameters [9]. On the other hand, the mentioned technology is normally utilized as a navigation and positioning system for marine vessels, thus, the idea is to use such a system, already available onboard, to obtain data useful for the estimation of some sea-state parameters.

In our specific application, the GNSS technology can be used for direct measurements of the wave height, through the so called GNSS Reflectometry (GNSS-R), as proposed by [10]. In that approach, the GNSS signals are received directly from the satellite and reflected by a surface, and they can be processed to obtain an altimetry measurement. In the recent years, this technique has been studied for various applications, such as soil moisture monitoring and sea state monitoring [11]. GNSS-R is used in various applications focused on sea state monitoring. In [12], the GNSS-R was used to measure the significant wave height and mean wave period studying the scattered signal of the Global Positioning System (GPS) in the band L1, that is, its main frequency band at 1575.42 MHz. The signal is reflected from the sea surface toward the antenna and compared to the data recorded by the near oceanographic buoy. The results show that coastal GNSS-R can be applied to sea state monitoring. Such attempts outcome from static coastal observations, but the same method was used on a shipboard, using an antenna and a receiver during navigation. In this case, results show a rather high correlation between the measured altitude and the significant wave height [13]. Another possibility is given by the Signal-to-Noise ratio (SNR). SNR information is part of the GNSS-observable quantities, and, in the marine environment, it oscillates due to the sea motion. A method based on the anisotropy of the attenuation of the SNR data to obtain sea wave direction is proposed in [14], where some experimentation is presented, using North Sea data.

In [15], a solid overview of the study on GNSS-based sea surface height (SSH) measurements in the Baltic Sea was provided. It highlights key findings, such as the differences between two methods for GNSS measurements: Continuously Operating Reference Stations (GNSS-CORS) and Precise Point Positioning (PPP). Results show the superiority of GNSS-CORS for short baselines (near the coast) and GNSS-PPP for longer distances. Another factor that emerges from [16], is the importance of the placement of the antenna on the vessel, for measuring the sea surface height. Results show how selecting the proper mode of measurement and the most suitable antenna position on the ship can influence the measurements.

Another study validates a GNSS-based sea level instrument which has been used for altimeter calibration, demonstrating its ability to map sea surface heights with high precision, maintaining a linear stability of 1 mm per m/s towing speed and achieving a sea surface slope accuracy better than 1 mm/km, with PPP processing, showing agreement with GNSS accuracy of the measurement mode at the 1–2 cm level [16].

Testing the GNSS potentialities in this field is rather complicated since, in real conditions [17], the only reference available is a certified wave buoy measurement. Dry conditions [18] can be more affordable, and even if they present some differences, they are suitable for a first test on the measurement systems and sensors. A dry buoy and sensor calibration device are proposed in [16]–[18]. A dry test is based on a motorized pendulum with two degrees of freedom. One axis enables the sensor or antenna holder to align with the Earth's gravity. The other is controlled and moves the pendulum according to wave height and period parameters. In the first reference, wave periods vary between 6 and 10 seconds, while in the second, they range from 11 to 15 seconds. The reference motion parameter can be obtained by the mechanical device itself, or by a reference sensor mounted together with the receivers under test. The wet test, on the other hand, involves placing the GNSS receiver on a moored wave buoy to compare the measurements. Such studies indicate that beside the altitude signal, the receiver's velocity signal can be suitable for measuring ocean waves.

In the present study, the proposed dry setup aims to integrate the advantages of previous experiments, introducing greater flexibility. The double-axis pendulum setup is retained, but now with only one controlled axis, while the second axis is free, leading to oscillations of the GNSS antenna stand, due to its inertia. Therefore, instead of moving vertically, while being perfectly aligned in the horizontal plane, the GNSS antenna experiences additional angular movements, simulating the slight shifts along the wave slope or small angular oscillations caused by vessel motion in real-world scenarios. Additionally, the verification process relies on an external, specialized, and previously calibrated IMU, directly providing heave measurements, thus reducing the dependence on the mechanical accuracy of the movement device.

The paper is organized as follows. Section 2 gives an overview on the GNSS, along with some details about its possible modes of operation and protocols, suitable for the present application. Section 3 presents the experimental setup and the instrumentation. Section 4 describes the data acquisition and processing procedures required to obtain the heave measurement. Then the method used to compare the results of the antennas with the reference is introduced. The results are presented in Section 5 and discussed in Section 6. Finally, conclusions are drawn in Section 7.

2. GNSS OVERVIEW

GNSS is a general term for a system that provides global positioning and timing services. With a compatible receiver, it enables users to determine their position at any location on the Earth. A set of Earth-orbiting satellites transmit signals with a time stamp and orbital data to final users equipped with a receiver, e.g. smartphone. The receiver, by processing the received satellite information, can compute the position of the

user. For an accurate positioning, it is required to receive signals from a minimum of four connected satellites, because it needs to solve four unknowns, such as latitude, longitude, altitude, and the receiver clock's offset, that is, the difference between the receiver's clock and the precise atomic clocks on the satellites. Each GNSS satellite transmits a signal, containing the precise time when the signal was sent, and the satellite's position in space, so the receiver calculates its distance from each satellite, using the time delay between the signal being sent and received. This process is called trilateration. Therefore, we can conclude that for each single unknown, we need at least one satellite to solve the equation accurately. Several applications use this technology, such as navigation, maritime, surveying, mapping, and environmental studies [19].

GNSS receivers can operate in different positioning modes, each having specific characteristics mainly regarding positioning accuracy. The following subsections will introduce three of the modes: Single Point (SP), Differential GNSS (DGNSS), and Real-Time Kinematic (RTK) modes.

2.1. Single Point mode

SP mode is a simple and cost-effective solution. Its simplicity comes from the fact that the GNSS receiver receives the signals directly from the satellite, without the need of any external corrections. This means that the positioning accuracy varies in the range of ± 3–10 m under normal conditions, such as the absence of atmospheric errors.

GNSS position accuracy is usually depicted by an accuracy circle, the radius of which is the distance between the mean measured position and the maximum deviation along the two coordinates. A set of measurements is typically considered statistically significant when it falls within a defined range, spanning from a minimum to a maximum value, corresponding to a position measurement duration of approximately five minutes.

The accuracy is rather large up to a few meters, nevertheless, it is sufficient for some applications, such as car and smartphone navigation, and sport activities [20]. Figure 1a shows the deviation of the antenna measurement in Single Point mode, with the antenna fixed in the installation point. Figure 1 enables the direct comparison of the three methods using the same graph scale, while Figure 2 presents a detailed view of the deviations for the DGNSS and the RTK.

2.2. Differential GNSS

DGNSS is an enhancement of the SP system, able to improve the positioning accuracy. This system is based on a network of fixed ground-based reference stations, which send position measurement corrections to the receivers. Ground stations compare their known position on the planet with the position measured by satellite signals, and transmit the required measurement corrections to the receiver, to reduce their errors mainly due to atmospheric disturbances and other factors [20], [21]. With this approach, accuracy decreases to less than one meter, as it is evident in Figure 1b, in comparison with the Single Point in Figure 1a. Detailed behaviour is presented in Figure 2a. It is worth noting that, in this case, the measuring system presents the complexity due to the specific connection to the base station, while previously the satellite receiver was sufficient.

2.3. Real-Time Kinematic mode

The RTK is a step forward respect to the DGNSS technique. Here, the accuracy is enhanced by receiving a set of corrections from a fixed base station. The base station is also a receiver that receives signals from two sources: the satellites and a ground base station that monitors the health of the satellites in their orbit. The general function of the DGNSS and the RTK modes is the same, with two main differences that affect the accuracy of measurement. The first difference regards the correction methods. DGNSS uses the so-called pseudo-range corrections, that is the distance between the satellite and the receiver, computed by measuring the time of flight of the signal. In this case, a known code is included in the transmission by the satellite, so that the receiver can compute the flight time. This kind of measurement is affected by some errors, such as clock errors and atmospheric delays, so the accuracy achieves ± 1–3 m. On the other hand, RTK uses carrier-phase corrections obtained from a reference station. The high-frequency GNSS carrier-phase is measured by counting the number of the full cycles and the fractional phase of the waves between the satellite and the receiver on the reference station [22]. The second difference between the methods regards the latency in sending the corrections. DGNSS presents a larger latency (a few seconds) compared to RTK that sends corrections to the receiver in real-time. The corrections are computed in a relation between the position of the fixed ground station and the position of the satellite in the orbit. As mentioned, the fixed station is placed in a known position, so it calculates the difference in relation to its position obtained from the satellite signals, estimating the satellite errors that constitute the correction to be transmitted to the receiver. Other types of corrections are also sent, for example the impact of the atmosphere on the quality of the signal. Overall, these corrections enable the receiver to enhance the accuracy of the position measurement to 1–2 cm [23]. To enable the GNSS receiver to use such RTK mode, it is necessary to connect the receiver to a nearby base station that transmits the Radio Technical Commission for Maritime Services (RTCM – subsection 2.4) corrections by the Networked Transport of RTCM via Internet Protocol (NTRIP, see subsection 2.5). Figure 1c shows the dramatic reduction as compared with SP and DGNSS, while details of the RTK deviations are presented in Figure 2b. As before, the observed deviation is obtained by measuring in RTK mode, on a fixed point.

2.4. RTCM corrections

RTCM is an international non-profit organization that develops standards for radio communications, navigation, and related technologies, particularly for maritime and GNSS applications [24].

RTCM SC-104 standard is one of their contributions to GNSS. This standard defines a protocol for transmitting GNSS correction data, which is commonly used for RTK and other high precision positioning methods. The standard specifies the content and organization of the messages for RTK correction, which can be sent by the base station to the rover receiver via radio, internet, or satellite communication, for computing an accurate position in real time. As subsection 2.3 described how the corrections are computed, the RTCM protocol here acts as a mediator to send the corrections from the base toward the rover.

2.5. NTRIP

NTRIP is a protocol for streaming GNSS correction data over the internet. It allows users to receive the RTK correction data from the base station remotely. It supports a client-server model divided into three components. The first component is the server that manages the distribution of the GNSS corrections, from the base station toward the receiver. The

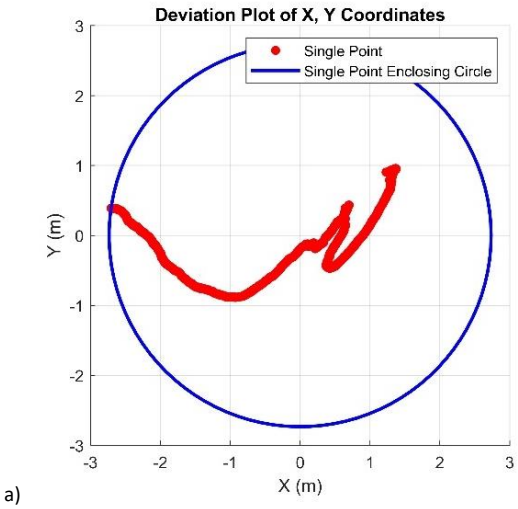

a)

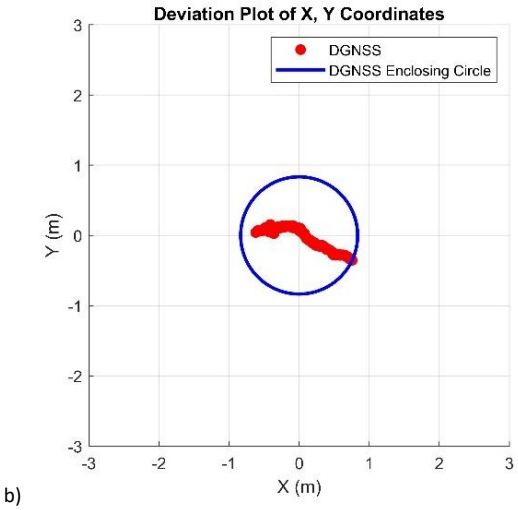

b)

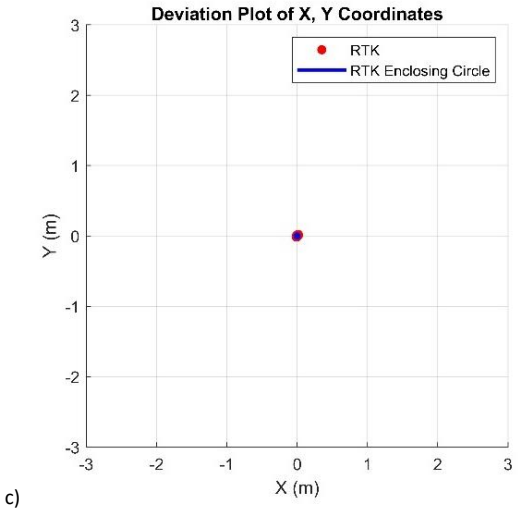

c)

Figure 1. The measurement deviation on a fixed point of the three different methods: a) SP, b) DGNSS, c) RTK.

second one is the base station that collects corrections and sends them to the server; typically, the base station is located at a known reference point. The last component is the client or the user that is connected to the server and receives the corrections in real time [25].

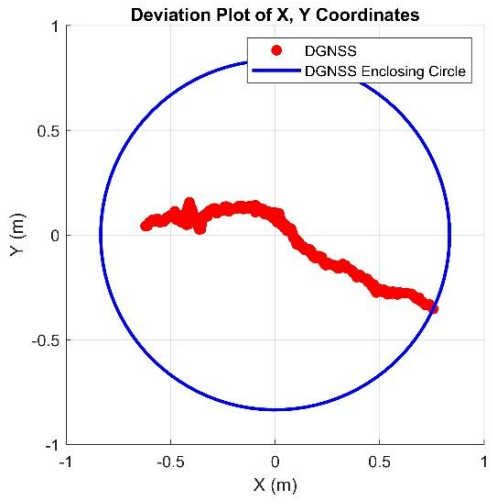

a)

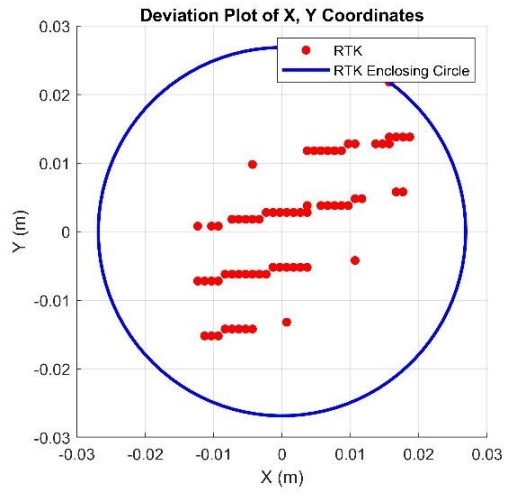

b)

Figure 2. The detailed view of the deviations of a) DGNSS and b) RTK.

3. EXPERIMENTAL SETUP

The aim of this paper is to test the ability of the GNSS signals for measuring ship motion. As depicted in the introduction, real condition testing in the sea is complex, mainly due to the lack of a precise reference and to the environmental conditions. Therefore, a dry test was designed to simulate real conditions in a controlled laboratory environment or dry outdoor environment. The main idea is to simulate a sea wave utilizing a pendulum that can generate wave-like movements. Firstly, the device and a specialized sensor for wave measurement were calibrated to characterize the ability to reproduce wave heave. Then, we installed GNSS antennas on the pendulum placed outdoor, so that we can record the satellite-based wave measurement, and the same measurement carried out by the reference specialized sensor. The following subsections are to introduce all the instruments used in this experiment.

3.1. Wave simulator

To simulate sea waves in dry conditions, it was required to create and design a proper, controllable motion generator. For this purpose, a pendulum was developed in the lab. The simulator is realized in non-ferromagnetic materials to be able to test inertial sensors in their full capability, including magnetometers [26]. The pendulum arm is a wood bar controlled

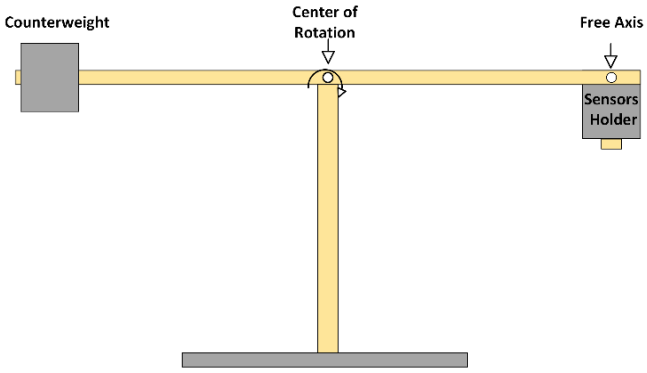

Figure 3. The scheme of the wave simulator in front view.

by a motor in its centre and carrying the sensor holder on one end. The sensor holder is attached to the pendulum by a free axis, allowing the movement of the sensor due to its dynamic inertia. That means the sensor holder is slightly moving away from the vertical direction during the wave motion, as it happens under real conditions. Figure 3 represents the scheme of the wave simulator in front view.

To install the GNSS antennas, another wood bar is attached under the sensor holder, which is perpendicular to the main wood bar, so the GNSS receiver antennas can be placed on it. The reference INS sensor introduced in subsection 3.2 is attached on the sensor holder. Figure 4 represents the scheme of the GNSS antennas and the INS installation on the wave simulator from top (a) and side (b) views.

3.2. Reference sensor

The validation of the pendulum generating the movement was caried out in a previous work [27], under an optoelectronic motion reconstruction system with a measuring uncertainty far below the required value for a wave monitoring system. In that occasion, the INS ELLIPSE-D, manufactured by SBG Systems, was also verified in [28], obtaining in the testing conditions a performance better than the one declared, within an average deviation of 1 mm and a standard deviation of 2 mm. On this basis, it is possible to consider such a sensor as a reference for

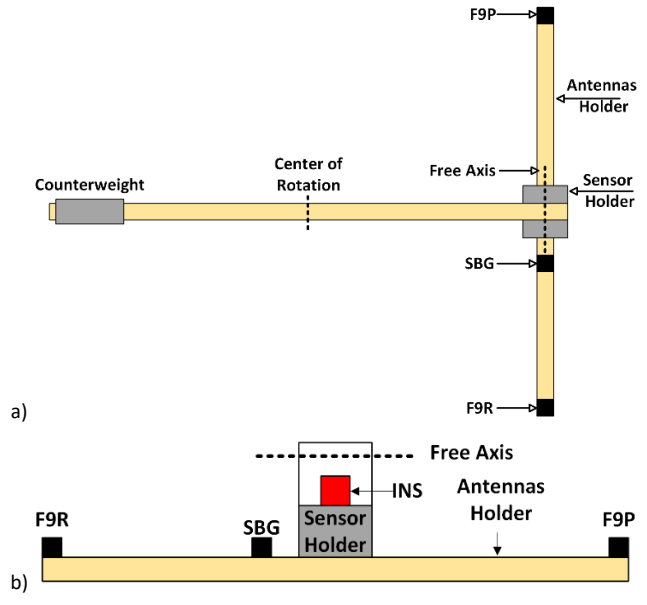

Figure 4. The schema of the GNSS antennas and INS installation in a) top and b) side views.

the measurements to be carried out by the simulator outdoor. The reference is a 9 Degrees of Freedom IMU, integrated with double GNSS antennas and a magnetometer. The internal firmware provides the displacement on the Z-axis (heave) with a nominal accuracy of 5 % [29]. Of course, antennas are disabled when operating indoor, while they can operate separately from the inertial sensor when operating outdoor. That is, we can consider it as a double sensor: a reference inertial system and a dual antenna GNSS receiver.

3.3. ZED-F9R

The ZED-F9R is a high-precision multi-band GNSS receiver with sensor fusion capabilities, manufactured by UBLOX [30]. It includes important features, such as the capability of centimetre-level accuracy with RTK positioning and also supports the RTCM protocols via internet or satellites. Another important feature is an integrated IMU for enhanced Dead Reckoning. This technique combines GNSS data with inertial data by sensor fusion, to maintain accurate location even in environments where the GNSS signals are weak or lost. In our specific application, the inertial measurement unit will not be used, since GNSS signals will be always available and in good condition, as generally happens in maritime applications.

3.4. ZED-F9P

The ZED-F9P is a multi-band GNSS receiver with RTK technology, which supports RTCM protocol obtaining centimetre-level accuracy position measurement within seconds. It is somewhat similar to the ZED-F9R, but with some differences. The ZED-F9P sampling rate is up to 25 Hz, but it could be configured as base and rover, while the ZED-F9R is up to 30 Hz, but it is only designed to be configured as rover. The significant difference is the Dead Reckoning technique that is the ability to combine GNSS data with an integrated IMU, to improve positioning accuracy in areas with poor satellite visibility. This technique is not available in ZED-F9P. This receiver is optimized for industrial navigation, robotics, UAVs, and automated machinery [30]. At the same time, it supports high update rate and low power consumption, which makes it ideal for dynamic applications, such as sea wave measurement or vessel movement measurement.

Summing up, the wave simulator carries four sensors for vessel motion measurement:

- a reference inertial sensor specialized for sea wave monitoring;
- a dual antenna GNSS receiver integrated in the reference but operated autonomously as a SP GNSS;
- a receiver type Z9P operating as RTK GNSS;
- a receiver type Z9R operating as DGNSS.

All the receivers provide beside positions.

4. METHODOLOGY

This section is divided into two sections. The first section is related to data acquisition procedures describing how each instrument is working during the test, and the second section describes the following data processing method.

4.1. Data acquisition

The main goal is to test receiver potentialities in measuring vessel motion, so the motion parameters must simulate sea conditions. The experiment considers four wave frequencies: 0.1, 0.15, 0.2, and 0.25 Hz, which, according to [31] and [32], usually occur in real sea environment. Each frequency is tested with

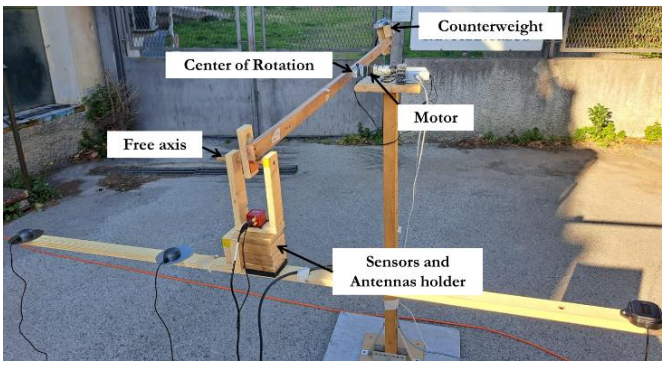

Figure 5. The real setup installation of the INS and GNSS antennas on the sensor holder for outdoor acquisition.

three increasing wave amplitudes, generated by the pendulum moving 20, 30, and 40 degrees. These three angles correspond to wave heights of 0.30 m, 0.45 m, 0.60 m, as measured by the reference sensor. To have some statistical robustness, each condition is repeated three times. A total of 36 trials was recorded. To set and control the motion parameters, the motor was connected to a LabVIEW software, as described in a previous work [27]. Figure 5 shows the real setup installation for outdoor acquisition.

The sampling rate was 10 Hz for all the receivers, but each one had a different internal mode of measurement for the GNSS antennas and for the software for controlling them. The SP GNSS was managed by its own software SBG CENTER [29], which is developed by the manufacturer, the SBG dual antenna was working as an SP mode of measurement. Although both UBLOX antennas were controlled and configured by U-CENTER [30] software, which is developed by UBLOX, they were working in different GNSS measuring modes: the ZED-F9P was working in RTK mode, while the ZED-F9R in DGNSS mode. The idea of the three different modes is to show the difference between the three modes, as well as the advantages and disadvantages of each mode; this aim is illustrated in more detail in the Results and Discussion sections.

Finally, the duration of each trial was designed to have an equal minimum amount of 48 wave periods at each testing frequency. This number was slightly reduced due to the synchronization process, obtaining a minimum of 40 wave periods. This is an important point which guarantees that the final processing of the data will have similar spectral measurement characteristics, while, at the same time, it creates some difficulties in testing, since at low wave frequencies (0.1 Hz) the trial lasts up to 8 minutes, while for the high wave frequency (0.25 Hz) its duration is up to 3.2 minutes. The acquisition length was previously assessed, when testing different inertial measurement units in [26]. Table 1 shows the selected frequencies and amplitudes applied in this experiment for all instruments.

Table 1. The selected frequencies and amplitudes applied in the experiment.

Frequency (Hz)	Amplitude (°)		
	20	30	40
0.1	X	X	X
0.15	X	X	X
0.2	X	X	X
0.25	X	X	X

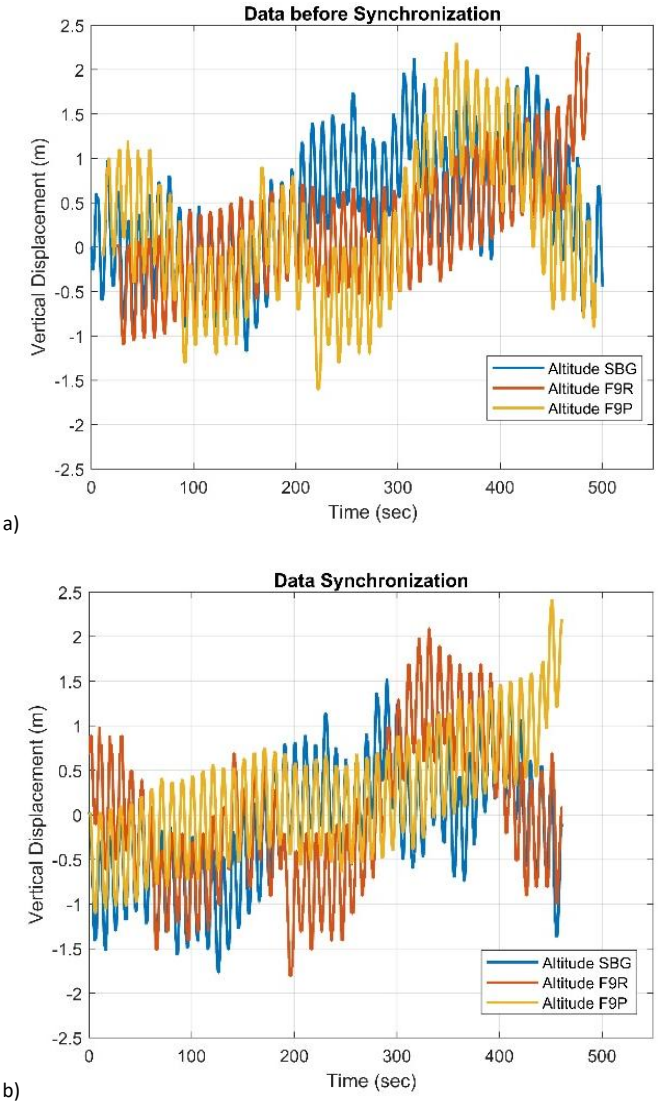

Figure 6. An example a) before and b) after data synchronization for the altitude signal between the instruments.

4.2. Data processing

To be able to compare data from the different sensors, it is firstly necessary to synchronize the acquisitions, after exporting the outputs of each independent instrument. The synchronization is based on the registration procedure used in the trials, which requires to first start the recording of the IMU-SP, then the ZED-F9P, and finally the ZED-F9R. The order of stops at the end of the trial is exactly the opposite, so the IMU-SP is always the longest data set and the ZED-F9R is the shortest one, see Figure 6a. The benefit from this procedure is to control the synchronization step easily and uniformly, with a standard processing code for all the tests. The synchronization is carried out considering the Universal Time Coordinates (UTC) that are recorded by each GNSS sensor. Considering the shortest data set, the start and end time are selected, then the same time coordinates are selected in the other sensor data sets, then the data sets are cut to have the same length. Figure 6a and b show an example of the data sets before and after the synchronization procedure, respectively.

Now, it is possible to process the data to obtain the vertical displacement. To this purpose, two strategies are available: the altitude measurement obtained directly from the GNSS receiver,

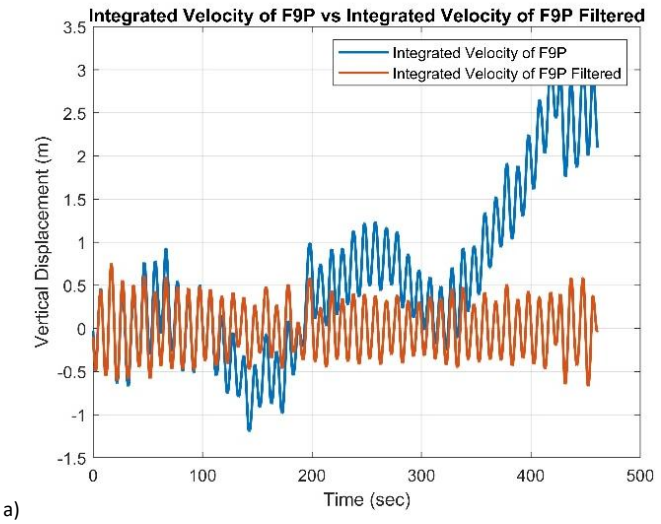

a)

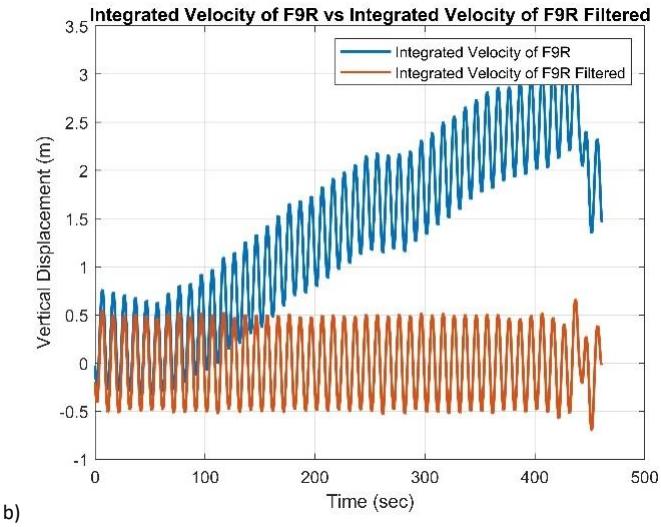

b)

Figure 7. The integrated velocity signal verses the filtered signal of a) the F9P and b) the F9R.

or the integration of the velocity obtained from the receiver. The former is certainly the simpler, requiring almost no processing, but the potentialities of the latter have also been investigated in the literature [26]–[28], even if it requires a time integration of the velocity signal.

Velocity integration presents the issue of the signal drift, which is always present, even if in a different amount. Since we are considering the measurement of a dynamic and periodic vertical motion, it is possible to isolate the quantity of interest by a proper high-pass filter. Thus, after velocity integration, a high-pass Butterworth filtering, with cut frequency placed at 0.03 Hz, is applied to remove this drift [26]. Some zero padding has been applied to improve the quality of the graphs. Figure 7a and b show an example of the integrated velocity signal of the F9P and F9R, and their filtered versions.

Now all the signals are ready to be compared. Since we are dealing with periodic motions, we decided to compare the amplitude spectra of the signals. The spectra are calculated without any tapering, not to reduce the information content in the signals or the spectral resolution. From each amplitude spectrum, the frequency and the amplitude of the main peak is extracted and compared between the three receivers of the two methods.

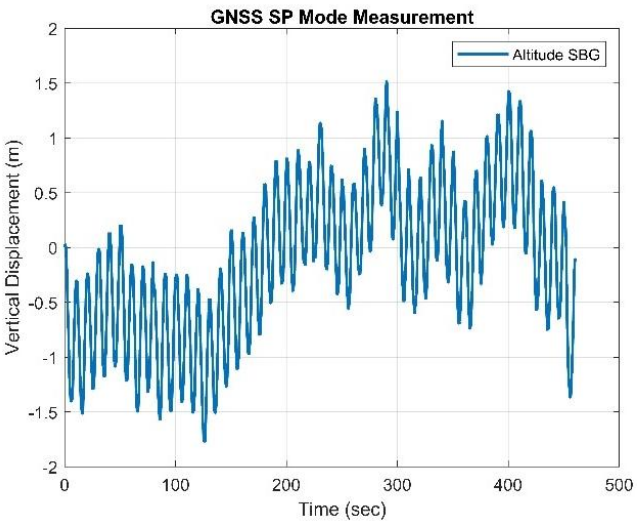

Figure 8. The recorded SBG altitude signal measured in SP mode.

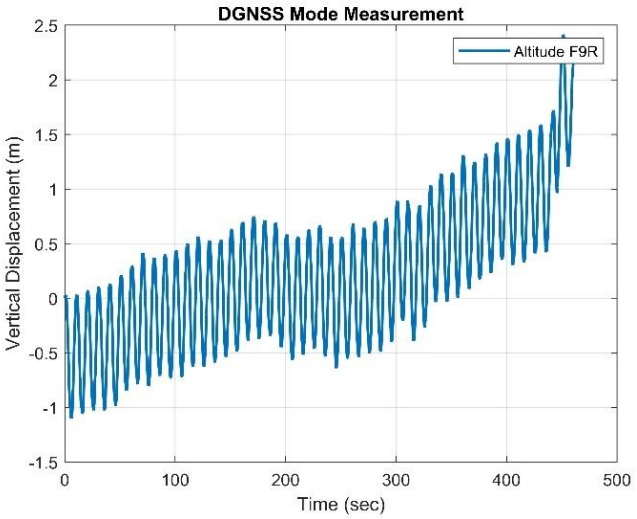

Figure 9. The recorded F9R altitude signal measured in DGNSS mode.

5. RESULTS

Firstly, an example of the data set from each receiver is presented to highlight the differences in the GNSS measuring mode.

Figure 8 shows the altitude signal for the receiver operating in SP mode. The SP mode has the lowest accuracy among the three considered modes, and even if the sensor has a rather high quality, the altitude measurements are not stable, and a waving is present in the signal. The well-known GNSS criticalities in altitude measurement are confirmed.

Figure 9 shows the altitude signal measured in the highly accurate DGNSS mode. The variations in altitude are clearly reduced compared to the SP mode, even if measurement data remain unstable.

The ZED-F9P receiver is working in RTK mode, receiving the RTCM corrections by the NTRIP via internet connection. This is certainly the most precise GNSS mode for positioning and also for altitude, as shown in Figure 10a. Unfortunately, its precision strictly depends on the received corrections, so if the connection is lost, the measurement is suddenly altered, coming

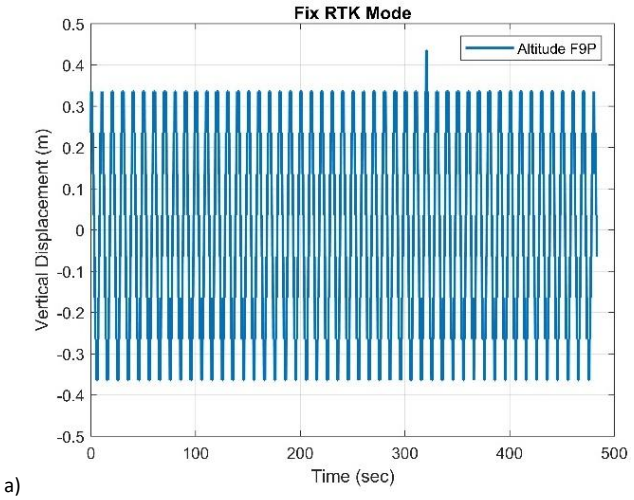

a)

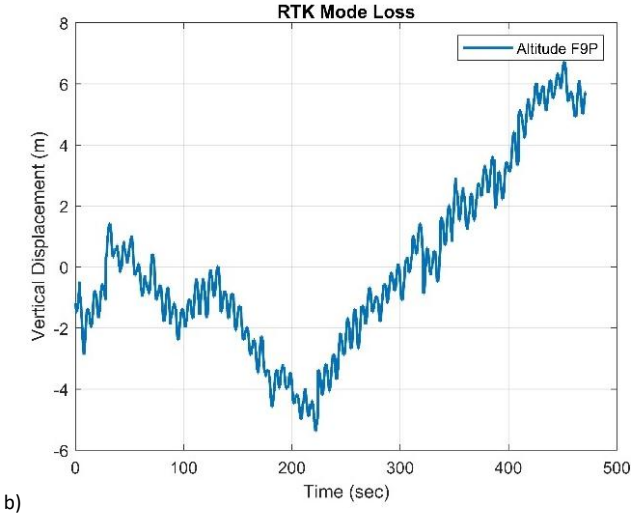

b)

Figure 10. a) The recorded F9P altitude signal measured in RTK mode with an ideal connection, b) the effect of an NTRIP connection loss on the measured altitude.

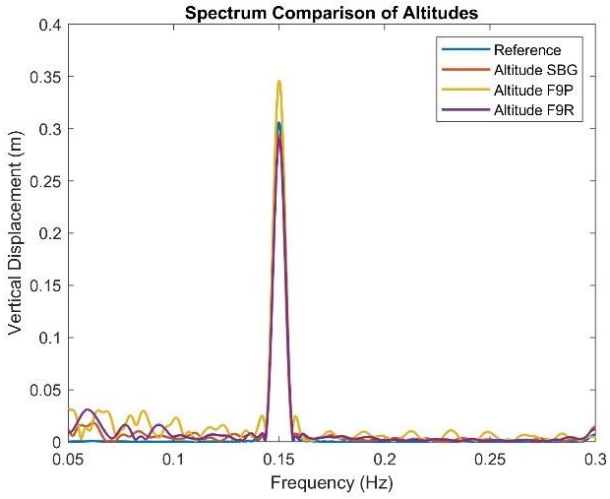

a)

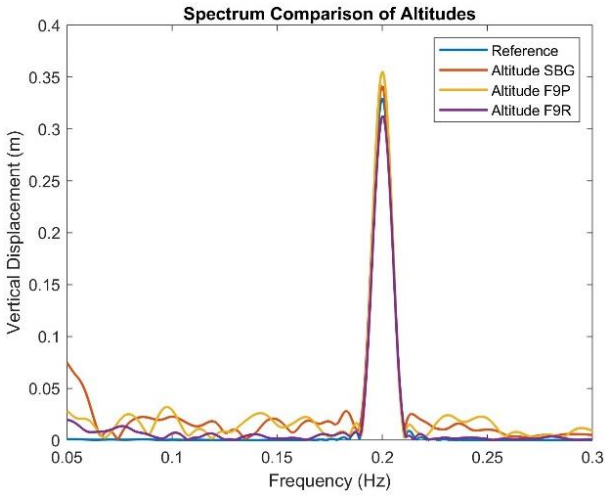

b)

Figure 11. The spectrum comparison of the altitude signals for two different test frequencies, a) 0.15 Hz and b) 0.2 Hz.

back to the original precision, when reconnected to the NTRIP. Figure 10b shows the effect of an NTRIP connection loss on the measured altitude.

This qualitative analysis confirms the quality of the RTK mode, but evidences some criticalities due to the NTRIP connection. The quantitative analysis considers the corresponding amplitude spectra. In the following figures, the spectra of the three receivers are considered, together with the reference signal from the specialized inertial sensor.

Figure 11 shows the spectrum comparison of the altitude signals for two different test frequencies. Figure 12 presents the spectrum comparison for the same tests considering the altitude obtained by velocity integration.

From each spectrum, it is possible to extract the position as the amplitude of the main peak. The position corresponds to the simulated wave frequency, and it is exactly determined by each method, without a significant difference. The amplitude corresponds to the simulated wave vertical height, or heave, and it is interesting to compare the results obtained by different sensors and measurement methods. Table 2 and Table 3 show the average amplitudes obtained at two different wave amplitudes during the three trials, taking into consideration that the results of a lost RTK connection are eliminated.

6. DISCUSSION

A discussion of the results is possible only in relation to the intended application. In fact, it is evident that SP and DGNSS mode give rather imprecise altitude measurements, see Figure 8 and Figure 9, while RTK seems somewhat better, see Figure 10a, even if less robust, due to the possible loss of the NTRIP connection, see Figure 10b.

When considering the specific application, the periodicity of the movements gives the possibility to improve results by proper filtering to isolate the periodicity in a suitable range for the application. In more detail, we can consider the deviation between the reference signal, the receiving modes, and the measuring method, based on direct altitude measurement or on velocity integration. The mean deviation over the repeated trials will represent an estimate of the measurement bias, and its standard deviation will represent the repeatability of the measurement method considered. Table 4 and Table 5 show the values for two movement amplitudes, taking into consideration that the results of a lost RTK connection are eliminated.

Figure 13 shows the same data graphically for all the test conditions, including the tests when the loss of the RTK connection occurred, to illustrate the difference of the efficiency of the RTK mode.

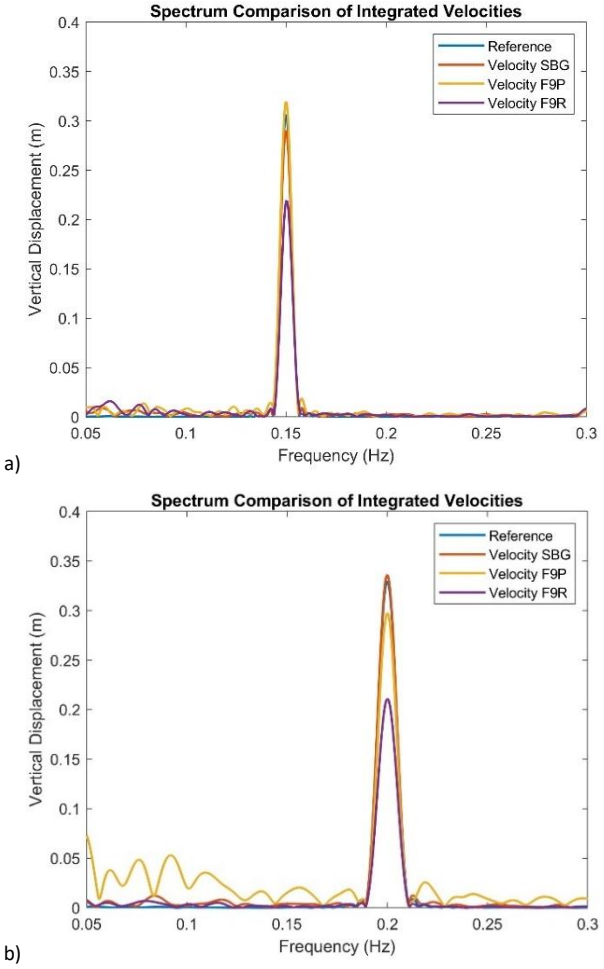

Figure 12. The spectrum comparison for the same test considering the altitude obtained by velocity integration, a) 0.15 Hz and b) 0.2 Hz.

Bias values range from -0.2 m up to 0.6 m, for both direct altitude measurement and velocity integration. For a better understanding of the situation, it is worth using relative deviation with respect to the reference sensor. For direct altitude measurement, the highest accuracy is obtained by the ZED-F9P receiver operating in RTK mode, with a 2.5 % mean deviation in all the tests with a good RTK connection. D-GNSS obtained 3.5 % and SP-GNSS obtained 4 %. This scenario confirms the well-known potentialities of the RTK-corrected GNSS measurement.

The situation is different when considering the same movement height measurement by velocity integration. Results show that the measurement obtained by the SBG SP-GNSS receiver is effective even if working in SP mode. This is possibly due to the Ekman filter that supports the precession velocity signal, obtaining higher precision results down to a resolution of mm/s, while for the other receivers, the resolution is limited to 10 mm/s, affecting the successive integration to obtain the vertical movement. Moreover, for the DGNSS and RTK modes of operation, the worst performance is due to the loss of the correction signals. Figure 14 shows such situations. In the overall evaluation, such results were discarded, obtaining an overall relative deviation of 2.5 %, 5 %, and 6 % for the SP, DGNSS and RTK, respectively. The results show that the SP-GNSS velocity-based height measurement is effective, since it can obtain relative deviations at the same level as an RTK direct altitude measurement. Moreover, SP-GNSS is by far the most robust approach, since the other two options require a dedicated connection to receive correction, and its loss can create unpredictable problems in the measurement.

Finally, considering the application we are focusing on, the relative deviation obtained in the tests is like the one typically specified for a specialized wave sensor, so the measurement accuracy obtained by GNSS seems to satisfy the application requirements.

Table 2. Average wave height amplitudes in meters at 20° oscillations.

Mode	Frequencies (Hz)			
	0.1	0.15	0.2	0.25
Reference	0.309	0.306	0.330	0.338
SP	0.319	0.314	0.299	0.341
DGNSS	0.338	0.326	0.349	0.362
RTK	0.285	0.338	0.316	0.314
SP Vel	0.322	0.318	0.301	0.328
DGNSS Vel	0.254	0.209	0.217	0.302
RTK Vel	0.327	0.318	0.304	0.297

Table 3. Average wave height amplitudes in meters at 40° oscillations.

Mode	Frequencies (Hz)			
	0.1	0.15	0.2	0.25
Reference	0.589	0.587	0.614	0.619
SP	0.591	0.572	0.673	0.587
DGNSS	0.578	0.596	0.594	0.579
RTK	0.587	0.563	0.584	0.603
SP Vel	0.572	0.585	0.533	0.579
DGNSS Vel	0.505	0.433	0.529	0.563
RTK Vel	0.524	0.537	0.573	0.568

Table 4. Amplitude measurement deviation: bias in meters and standard deviation in meters for minimum amplitude movement 20°.

Frequencies (Hz)	0.1		0.15		0.2		0.25	
Mode	bias	Std	Bias	Std	Bias	Std	Bias	Std
SP	0.018	0.008	0.008	0.002	-0.042	0.014	0.003	0.008
DGNSS	0.023	0.006	0.025	0.005	0.031	0.003	0.026	0.003
RTK	0.018	0.005	-0.064	0.002	-0.026	0.026	0.297	0.018
SP Vel	0.012	0.003	0.032	0.002	-0.022	0.022	-0.015	0.013
DGNSS Vel	0.051	0.001	0.084	0.003	0.108	0.004	0.148	0.004
RTK Vel	-0.014	0.003	0.032	0.07	0.043	0.027	0.268	0.03

Table 5. Amplitude measurement deviation: bias in meters and standard deviation in meters for maximum amplitude movement 40°.

Frequencies (Hz)	0.1		0.15		0.2		0.25	
Mode	bias	Std	Bias	Std	Bias	Std	Bias	Std
SP	0.002	0.007	0.002	0.011	-0.067	0.003	0.078	0.004
DGNSS	0.024	0.019	0.017	0.018	0.022	0.005	0.014	0.009
RTK	-0.013	0.029	-0.008	0.026	0.552	0.039	0.034	0.013
SP Vel	0.023	0.021	0.015	-0.014	-0.083	0.006	0.077	0.005
DGNSS Vel	0.124	0.017	0.104	0.011	0.217	0.019	0.229	0.053
RTK Vel	0.121	0.058	0.123	0.064	0.032	0.01	0.421	0.117

7. CONCLUSIONS

The conducted experiment successfully evaluated the effectiveness of GNSS signals in measuring vertical displacement (heave) through a controlled pendulum motion setup. The study

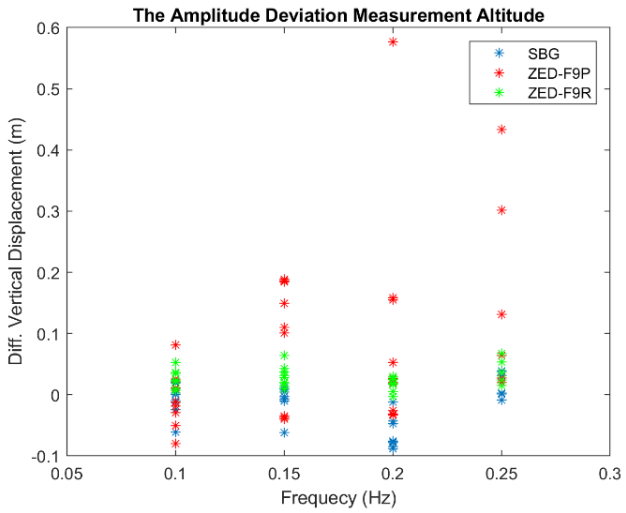

Figure 13. The deviations of the amplitude of the altitude of all tests.

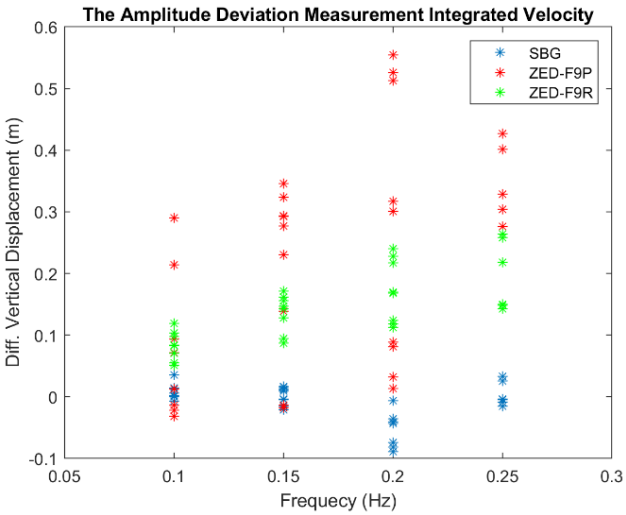

Figure 14. The deviations of the amplitude of the integrated velocity of all tests.

incorporated various measurement modes—SP, DGNSS, and RTK, using different GNSS antennas and an INS system as a reference. The results demonstrated that GNSS-based velocity measurements can be effective for heave estimation, provided there is sufficient precision in velocity recording and correction signal stability.

The RTK mode exhibited the highest accuracy among the GNSS antennas, with a deviation of 2.5 % for the altitude signal, compared to the reference INS measurements. The DGNSS mode (ZED-F9R) followed with a 3.5 % deviation, while the SP mode (SBG) showed the least accuracy with 4 %. Similarly, altitude-based heave estimations showed a deviation of 2.5 %, 5 %, and 6 % for the RTK, DGNSS, and SP modes, respectively. A key challenge encountered was the loss of NTRIP correction in the RTK mode, affecting measurement stability.

Overall, while GNSS-based measurements demonstrated potential for heave estimation, further improvements in velocity precision and correction signal reliability are necessary to enhance accuracy. The study highlights the importance of considering GNSS measurement modes and processing techniques to achieve reliable results in marine motion applications.

REFERENCES

[1] G. B. Rossi, A model for indirect measurement, Measurement, vol. 214, 2023, p. 112798.
DOI: 10.1016/j.measurement.2023.112798

[2] G. B. Rossi, A. Cannata, A. Iengo, M. Migliaccio, G. Nardone, V. Piscopo, E. Zambianchi, Measurement of sea waves, Sensors, vol. 22, 2021, no. 1, p. 78.
DOI: 10.3390/s22010078

[3] A. H. Brodtkorb, U. D. Nielsen, A. J. Sørensen, Sea state estimation using vessel response in dynamic positioning, Applied Ocean Research, vol. 70, 2018, pp. 76–86.
DOI: 10.1016/j.apor.2017.09.005

[4] G. B. Rossi, G. Vernengo, F. Crenna, F. Soardi, M. Khalil, A new approach to the estimation of sea state based on shipboard observations – preliminary results, IEEE Int. Workshop on Metrology for the Sea; Learning to Measure Sea Health Parameters (MetroSea), Portorose, Slovenia, 14-16 October 2024, pp. 342–346.
DOI: 10.1109/MetroSea62823.2024.10765784

[5] U. D. Nielsen, The wave buoy analogy—estimating high-frequency wave excitations, Applied Ocean Research, vol. 30, 2008, no. 2, pp. 100–106.
DOI: 10.1016/j.apor.2008.07.002

[6] T. Zhang, Z. Ren, Restricted isometry property in wave buoy analogy and application to multispectral fusion, IEEE Transactions on Intelligent Transportation Systems, 2025.
DOI: 10.1109/TITS.2024.3519199

[7] A. H. Brodtkorb, U. D. Nielsen, A. J. Sørensen, Sea state estimation using model-scale DP measurements, OCEANS 2015-MTS/IEEE Washington, Washington, DC, USA, 19-22 October 2015, pp. 1–7.
DOI: 10.23919/OCEANS.2015.7404402

[8] J. Li, L. Li, X. Wen, A novel method of estimating ship heave motion based on dual inertial measurement units, Journal of Physics: Conference Series, IOP Publishing, 2022, vol. 2183, no. 1, p. 012002.
DOI: 10.1088/1742-6596/2183/1/012002

[9] J. De Vries, J. Waldron, V. Cunningham, field tests of the new datawell DWR-G GPS wave buoy, Sea Technology, vol. 44, 2003, no. 12, pp. 50–55. Online [Accessed 19 June 2025].
https://datawell.nl/wp-content/uploads/2022/08/datawell_publication_dwr-g_seatechnology.pdf

[10] M. Martin-Neira, A Passive Reflectometry and Interferometry System (PARIS): Application to ocean altimetry, ESA journal, vol. 17, 1993, no. 4, pp. 331–355.

[11] Y. Yang, Y. Zheng, W. Yu, W. Chen, D. Weng, Deformation monitoring using GNSS-R technology, Advances in Space Research, vol. 63, 2019, no. 10, pp. 3303–3314.
DOI: 10.1016/j.asr.2019.01.033

[12] F. Soulat, M. Caparrini, O. Germain, P. Lopez-Dekker, M. Taani, G. Ruffini, Sea state monitoring using coastal GNSS-R, Geophysical Research Letters, vol. 31, 2004, no. 21.
DOI: 10.1029/2004GL020680

[13] O. Roggenbuck, J. Reinking, T. Lambertus, Determination of significant wave heights using damping coefficients of attenuated GNSS SNR data from static and kinematic observations, Remote Sensing, vol. 11, 2019, no. 4, p. 409.
DOI: 10.3390/rs11040409

[14] J. Reinking, O. Roggenbuck, G. Even-Tzur, Estimating wave direction using terrestrial GNSS reflectometry, Remote Sensing, vol. 11, 2019, no. 9, p. 1027.
DOI: 10.3390/rs11091027

[15] A. Liibusk, S. Varbla, A. Ellmann, K. Vahter, R. Ui- boupin, N. Delpeche-Ellmann, Shipborne GNSS acquisition of sea surface heights in the Baltic Sea, Journal of Geodetic Science, vol. 12, 2022, no. 1, pp. 1–21.
DOI: 10.1515/jogs-2022-0131

[16] P. Bonnefond, O. Laurain, P. Exertier, M. Calzas, T. Guinle, N. Picot, F. P. Team, Validating a new GNSS-based sea level

instrument (CalNaGeo) at Senetosa Cape, Marine Geodesy, vol. 45, 2022, no. 2, pp. 121–150.
DOI: 10.1080/01490419.2021.2013355

[17] G. Joodaki, H. Nahavandchi, K. Cheng, Ocean wave measurement using GPS buoys, Journal of Geodetic Science, vol. 3, 2013, no. 3, pp. 163–172.
DOI: 10.2478/jogs-2013-0023

[18] D.-J. Doong, B.-C. Lee, C. C. Kao, Wave measurements using GPS velocity signals, Sensors, vol. 11, 2011, no. 1, pp. 1043–1058.
DOI: 10.3390/s110101043

[19] NovVatel, GPS & GNSS Equipment, Products & Solutions Website. Online [Accessed 19 June 2025].
https://www.novatel.com

[20] N. Crocetto, M. Gatti, N. Perfetti, The GPS single point positioning: a data processing program for tutorial purposes, Int. Archives of Photogrammetry and Remote Sensing, vol. 32, 1997, pp. 131–135. Online [Accessed 23 September 2025]
https://isprs.org/proceedings/XXXII/6-W1/131_XXXII-6-W1.pdf

[21] European Space Agency, Website. Online [Accessed 19 June 2025]
https://www.esa.int/

[22] E. D. Kaplan, C. Hegarty, Understanding GPS/GNSS: principles and applications, Artech House, ISBN: 978-1-63081-058-0, 2017.

[23] R. Leandro, H. Landau, M. Nitschke, (+ 14 more authors), RTX Positioning: The Next Generation of cm-accurate Real-time GNSS Positioning, Proc. of the 24th Int. Technical Meeting of the Satellite Division of the Institute of Navigation (ION GNSS 2011), Portland, OR, USA, 20-23 September 2011, pp. 1460–1475. Online [Accessed 23 September 2025]
https://www.ion.org/publications/abstract.cfm?articleID=9705

[24] Radio Technical Commission for Maritime Services, Website. Online [Accessed 19 June 2025].
https://www.rtcm.org/

[25] Federal Agency for Cartography and Geodesy of Germany, Website. Online [Accessed 23 September 2025]
https://www.bkg.bund.de/

[26] M. Khalil, F. Crenna, G. B. Rossi, Wave heave sensor verification in dry conditions with optoelectronic reference, Acta IMEKO, vol. 13, 2024, no. 4, pp. 1–10.
DOI: 10.21014/actaimeko.v13i4.1768

[27] F. Crenna, G. B. Rossi, M. Khalil, Calibration of sensors for indirect sea-wave measurement: Experimental aspects, Measurement: Sensors, 2024, p. 101524.
DOI: 10.1016/j.measen.2024.101524

[28] M. Khalil, F. Crenna, G. B. Rossi, GNSS signals for sea wave measurements, IEEE Int. Workshop on Metrology for the Sea, Learning to Measure Sea Health Parameters (MetroSea), Portorose, Slovenia, 14-16 October 2024, pp. 329–333.
DOI: 10.1109/MetroSea62823.2024.10765644

[29] SBG Systems, Website. Online [Accessed 19 June 2025].
https://www.sbg-systems.com

[30] Ublox, Website. Online [Accessed 19 June 2025].
https://www.u-blox.com/

[31] W. H. Munk, Origin and generation of waves, Coastal Engineering Proceedings, 1950, no. 1, pp. 1–1.

[32] B. Kinsman, Wind waves: their generation and propagation on the ocean surface, Courier Corporation, 1984.